Available online at www.sciencedirect.com
SCIENCE DIRECT®
Journal of Solid State Chemistry 177 (2004) 4420–4427
JOURNAL OF SOLID STATE CHEMISTRY
www.elsevier.com/locate/jssc

A structural study of the perovskite series $Ca_{1-x}Na_xTi_{1-x}Ta_xO_3$

Roger H. Mitchell*, Ruslan P. Liferovich[1]

Department of Geology, Lakehead University, 955 Oliver Road, Thunder Bay, Ont., Canada P7B 5E1

Received 9 July 2004; received in revised form 3 September 2004; accepted 9 September 2004

Abstract

Compounds in the solid solution series $Ca_{1-x}Na_xTi_{1-x}Ta_xO_3$ were synthesized at 1300 °C, followed by annealing at 850 °C or 800 °C with quenching and/or slow cooling to room temperature. Rietveld refinement of their powder X-ray diffraction patterns show that all compounds are single-phase ternary perovskites which adopt the space group *Pbnm* ($a \approx b \approx \sqrt{2}a_p$; $c \approx 2a_p$; $Z=4$) at ambient conditions. The unit cell parameters and cell volumes of the compounds increase regularly with increasing values of x. The coordination of the *A*-site cations changes throughout the series from eight for $CaTiO_3$ to nine for $NaTaO_3$. Compounds with $0 \leqslant x \leqslant 0.4$ have *A*-site cations in eight fold coordination, whereas the coordination of those with $0.4 < x < 0.9$ is ambiguous. Analysis of the crystal chemistry of the compounds shows that the change in coordination at $x=0.4$ is related to the departure of the *B*-site cations from the second coordination sphere of the *A*-site cations, as in compounds with $x>0.4$ the A–^{II}O distances become less than the *A–B* intercation distances. Contemporaneous with these coordination changes, the tilt angles of the BO_6 polyhedra decrease with increasing values of x. This solid solution series is unusual in that these structural and coordination changes occur regardless that Goldschmidt tolerance factors remain essentially constant at approximately 0.89, and observed tolerance factors, assuming eight fold coordination of the *A*-site cations, range only from 0.91 to 0.93 ($0 \leqslant x \leqslant 0.8$).

Keywords: Perovskite; Calcium titanate; Sodium tantalate; Powder X-ray diffraction; Rietveld refinement; Coordination analysis

1. Introduction

The structure of $CaTiO_3$, i.e. perovskite (*sensu stricto*) has been studied extensively as a function of temperature and pressure [1–4]. At ambient conditions the compound adopts the orthorhombic space group *Pnma* (#62), although the unconventional *Pbnm* (#62; *cab*) setting with $a \approx b \approx \sqrt{2}a_p$, $c \approx 2a_p$, $Z=4$ is typically used to describe the unit cell dimensions [1,5]. The structures of ABO_3 orthoperovskites, e.g. $CaTiO_3$ and $GdFeO_3$ [6], are derived from a cubic $Pm\bar{3}m$ aristotype, such as $SrTiO_3$ [7], by tilting of the BO_6 octahedra about the [010], [001] and [111] axes of the cubic subcell (Fig. 1). The distortion of the BO_6 framework arises because of the poor geometrical fit of cations which are smaller than Sr^{2+} into the *A*-site. The octahedron tilting scheme for the space group *Pbnm* expressed in the notation of Glazer [8] is $a^-a^-c^+$.

Solid solutions of $CaTiO_3$ with $SrTiO_3$ have been studied extensively [9–13], and have concluded [10] that the series of phase transitions with increasing Sr content in the series $Ca_{1-x}Sr_xTiO_3$ is from *Pbnm* through $I4/mcm$ to $Pm\bar{3}m$. Importantly, this sequence mirrors the series of phase transitions observed for $CaTiO_3$ with increasing temperature [2,3].

Sodium tantalate, $NaTaO_3$, is isostructural with $CaTiO_3$ at ambient conditions. However, with increasing temperature, $NaTaO_3$ does not undergo the same series of phase transitions as found for $CaTiO_3$. Thus, the room temperature *Pbnm* structure transforms through orthorhombic *Cmcm* (700 K) and tetragonal $P4/mbm$ (835 K) structures before becoming cubic above 890 K [13,14].

It has been shown [5,6] that the coordination polyhedron of the cations occupying the *A*-site of most

*Corresponding author. Fax: 807-346-7853.
E-mail address: rmitchel@lakeheadu.ca (R.H. Mitchell).
[1]*Permanent address*: Geological Institute Kola Science Centre, Russian Academy of Science, 14 Fersman Str., Apatity 184200, Russia.

0022-4596/$ - see front matter © 2004 Elsevier Inc. All rights reserved.
doi:10.1016/j.jssc.2004.09.031

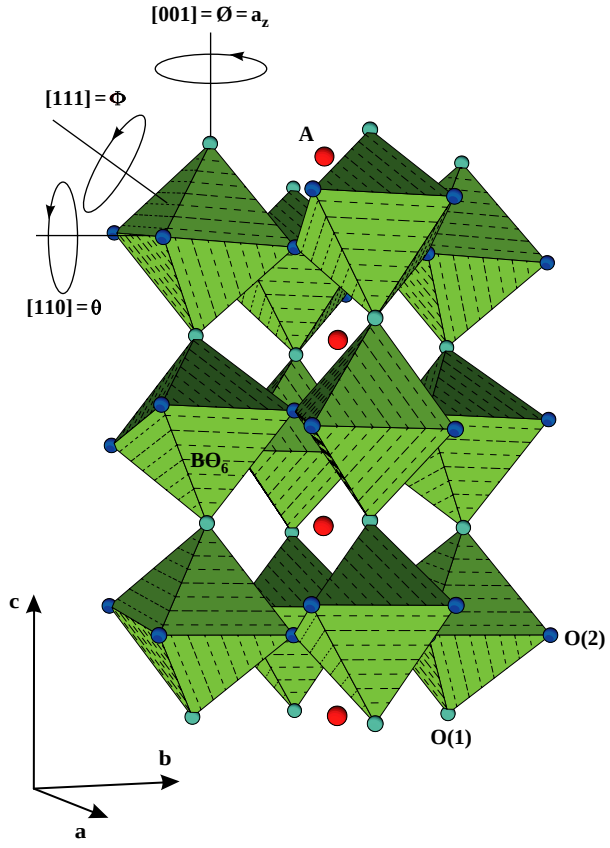

Fig. 1. Crystal structure of the orthorhombic $Ca_{1-x}Na_xTi_{1-x}Ta_xO_3$ solid solution series; Ø, θ, and Φ denote BO_6 octahedron tilting about $[001]_p$, $[110]_p$, and $[111]_p$, respectively. *A* is an eight- or nine-fold coordinated cation in the *A*-site.

ABO_3 orthoperovskites is best regarded as eight-fold (^{viii}A), rather than 12-fold (^{xii}A), i.e., a four-fold antiprism with $2 \times O(1)$ and $6 \times O(2)$ bonds, rather than a cubo-octahedron. This coordination arises because the rotation of the BO_6 octahedra to compensate for the poor dimensional fit of the cations occupying the *A*-site results in the degeneration of the 12 *A*–O bonds to eight short A–$^{I}O(1,2)$ and four long A–$^{II}O(2)$ bonds, giving rise to the first (I) and second (II) coordination spheres of the *A*-site cations [6]. The degeneration of the coordination sphere reflects the antipathetic evolutionary trends of the *A*-site bond lengths in the first and second coordination spheres. Typically, the distortion of the AO_8 coordination polyhedron in orthoperovskites is also accompanied by displacement of the *A*-site cation from the center of the polyhedron. Bond valence analysis [16,17] and crystal structure determinations of $A^{2+}B^{4+}O_3$ and $A^{3+}B^{3+}O_3$ orthoperovskites [5,6,18] show that, in most compounds, some or all four of the A–$^{II}O(2)$ bonds exceed the *A*–*B* intercation distances. Thus, in $CaTiO_3$, the *B*-site cation (Ti^{4+}) enters the second coordination sphere of the ^{viii}A atom (Ca^{2+}) because the longest A–$^{II}O(2)$ bonds exceed the shortest *A*–*B* distances. In contrast, crystal structure data for $NaTaO_3$ [14,15], an $A^{+}B^{5+}O_3$ orthoperovskite, indicate that the Ta atom lies outside of the second coordination sphere of ^{viii}Na at ambient conditions.

There have been no structural studies of the solid solution series between $CaTiO_3$ and $NaTaO_3$. If, as noted above, composition-driven phase transformations mirror those induced by temperature change, we might expect structural complexity in the $CaTiO_3$–$NaTaO_3$ solid solution series, as the tetragonal structures observed for the pure compounds at high temperature result from single antiphase ($I4/mcm$; $a^oa^oc^-$) and inphase ($P4/mbm$; $a^oa^oc^+$) tilts, respectively. In addition, we can expect to observe changes in the interaction of the *B*-site cation with the second coordination sphere as a function of composition, as solid solution from $CaTiO_3$ towards $NaTaO_3$ represents an increase in the average ionic radius (*R*) of the *A* ($^{viii}R_A$) and *B* ($^{vi}R_B$) sites together with an increase in coordination number from eight to nine.

2. Experimental

Compositions corresponding to the $Ca_{1-x}Na_xTi_{1-x}Ta_xO_3$ solid solution series were synthesized from stoichiometric amounts of high-purity grade Na_2CO_3, $CaCO_3$, TiO_2, Ta_2O_5 (all 99.99% pure compounds from Aldrich Chemical Co.). Na_2CO_3 was added in 10 mol% excess to all starting mixtures to compensate for volatilization of sodium. All reagents were dried at 120 °C and mixed in an agate mortar under acetone, followed by calcination in air for 24 h at 1000 °C. After regrinding, the samples were pelletized at a pressure of 10 tons per square centimeter, and then heated in air for two days at 1300 °C and quenched. All samples were then annealed for two days at 800 °C and then re-quenched.

Refinement of powder X-ray diffraction data obtained for samples quenched after 48 h—annealing at 800 °C, demonstrated the presence of single phase *Pbnm*-structured compounds for the compositions with $0 \leqslant x \leqslant 0.8$. In contrast, $NaTaO_3$ and $Ca_{0.1}Na_{0.9}Ti_{0.1}Ta_{0.9}O_3$ formed under the same conditions were shown to consist of both *Pbnm*- and *Cmcm*-structured phases. As sodium tantalate (V) has been shown to adopt the space group *Cmcm* from 485 to 565 °C [14,15], we considered that the *Cmcm* phase must represent a metastable pinned high-temperature structure. To eliminate these metastable phases we undertook further annealing of $NaTaO_3$ and $Ca_{0.1}Na_{0.9}Ti_{0.1}Ta_{0.9}O_3$ at 850 °C (6 h) and 500 °C (6 h), followed by slow cooling at a rate of 1 °C per minute to ambient temperature. As a result, single phase *Pbnm*-structured modifications were obtained for both of these samples, as confirmed by

Rietveld analysis of their powder X-ray diffraction patterns.

Step-scanned X-ray diffraction (XRD) powder patterns of the products were obtained at room temperature using a Philips 3710 diffractometer (Cu$K\alpha$ radiation; 2θ range 10–145°; $\Delta 2\theta$ step 0.02°; time per step 4 s; graphite monochromator).

The XRD patterns were inspected using the Bruker AXS software package EVA to identify the phases present and confirm that perovskite-structured compounds were formed. Data were further analysed by Rietveld methods using the Bruker AXS software package TOPAS 2.1 operated in the fundamental parameters mode [19]. Data were corrected for Lorenz and polarization effects. Refined parameters included: zero corrections; scaling factors; cell dimensions; atomic positional coordinates; preferred orientation corrections; crystal size and strain effects; and isotropic thermal parameters (B_{iso}). Fig. 2 is a Rietveld refinement plot for $Ca_{0.3}Na_{0.7}Ti_{0.3}Ta_{0.7}O_3$.

The ATOMS-6.0 software package [20] was used to determine interaxial angles describing the distortion of BO_6 octahedra, i.e., the B–O(1)–B and B–O(2)–B angles. The IVTON program [21] was employed to characterize the coordination spheres of A and B cations, obtain bond lengths, volumes of coordination polyhedra and displacements of cations from the centers of coordination polyhedra. Tilt angles of BO_6 octahedra were calculated from bond angles following Zhao et al. [22].

The compositions of samples were assessed by X-ray energy-dispersion spectrometry using a JEOL JSM-5900 scanning electron microscope equipped with a LINK ISIS 300 analytical system incorporating a Super ATW Element Detector (133 eV FwHm MnK). Experimental products do not contain any contaminant phases, are stoichiometric, and homogeneous within the accuracy of the microprobe technique.

3. Results and discussion

The complete perovskite-structured $Ca_{1-x}Na_x Ti_{1-x}Ta_xO_3$ ($0 \leqslant x \leqslant 1$) solid solution series was synthesized and is stable at ambient conditions. Using ionic radii (R) given by Shannon [23], the mean $^{viii}R_A$ of the compounds formed increases from 1.12 to 1.18 Å, and the mean $^{vi}R_B$ increases from 0.605 to 0.64 Å for the $CaTiO_3$ and $NaTaO_3$ end members, respectively. Throughout the series the Goldschmidt tolerance factor (t) [24] increases only slightly from 0.887 to 0.892 (Table 1). The crystallographic characteristics of the $Ca_{1-x}Na_xTi_{1-x}Ta_xO_3$ series are given in Table 1, crystallochemical parameters in Table 2, and selected interatomic distances and angles in Table 3.

The cell dimensions and fractional atomic coordinates obtained for $CaTiO_3$ and $NaTaO_3$ end members of the solid solution series are close to those previously reported for their analogs at ambient conditions [1,3,14,15]. Fig. 3 shows that the unit cell parameters and unit cell volume regularly increase with x throughout the $Ca_{1-x}Na_xTi_{1-x}Ta_xO_3$ series due to the replacement of $^{viii}Ca^{2+}$ and $^{vi}Ti^{4+}$ by the larger $^{viii}Na^{+}$ and $^{vi}Ta^{5+}$ cations. All of the samples have $a < c/\sqrt{2} < b$ (Fig. 3) and $V_{A12}/V_B < 5$ (Table 2). Such "non-reversed" lattice parameters suggest that distortions of the coordination polyhedra are sufficient to overcome the changes in the a-dimension resulting from octahedron tilting [5].

As expected for most of the Ca-rich ($x < 0.4$) orthorhombically distorted perovskite structures, the A-site coordination polyhedron is a four-fold antiprism with the A-site cation in eight-fold coordination. Bond length analysis shows that B-site cation leaves the second coordination sphere of the A cations when x exceeds 0.4 (Fig. 4a). This observation is robust as the estimated standard deviations of the bond lengths are far less than the differences in bond length between

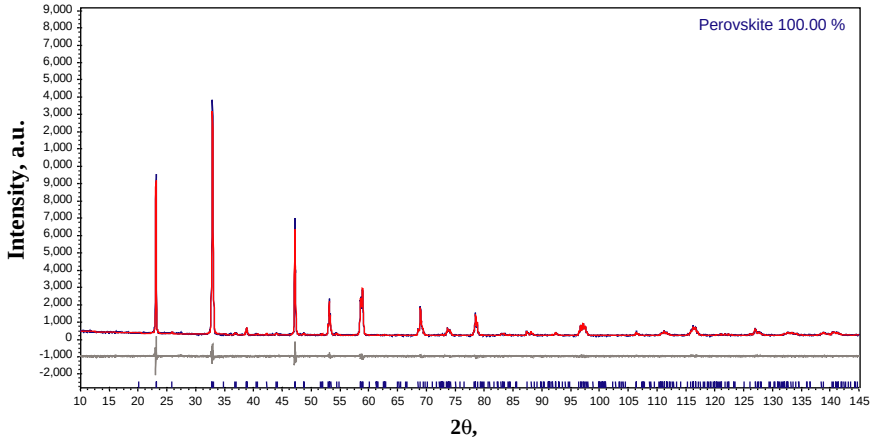

Fig. 2. Rietveld refinement plot of the powder diffraction data for $Ca_{0.3}Na_{0.7}Ti_{0.3}Ta_{0.7}O_3$. The bars indicate the allowed Bragg reflections for *Pbnm* structure. For details of the refinement, see text and Table 1.

Table 1
Crystallographic characteristics of $Ca_{1-x}Na_xTi_{1-x}Ta_xO_3$

	$CaTiO_3$	$x = 0.1$	$x = 0.2$	$x = 0.3$	$x = 0.4$	$x = 0.5$	$x = 0.6$	$x = 0.7$	$x = 0.8$	$x = 0.9$	$NaTaO_3$
$^{viii}R_A$	1.120	1.126	1.132	1.138	1.144	1.150	1.156	1.162	1.168	1.174	1.180
$^{vi}R_B$	2.864	2.869	2.874	2.879	2.884	2.889	2.893	2.898	2.903	2.908	2.913
t	0.887	0.888	0.888	0.889	0.889	0.890	0.890	0.891	0.891	0.892	0.892
$^{viii}t_o$	0.912	0.908	0.915	0.915	0.916	0.924	0.927	0.925	0.934	0.927	0.936
a (Å)	5.38159(6)	5.39461(8)	5.40650(8)	5.41652(9)	5.42689(8)	5.43749(8)	5.44901(11)	5.45831(10)	5.46568(9)	5.47344(8)	5.48109(9)
b (Å)	5.44281(7)	5.45274(8)	5.46125(9)	5.46935(9)	5.47740(8)	5.48508(8)	5.49243(11)	5.50015(10)	5.50893(9)	5.51680(8)	5.52351(9)
c (Å)	7.64207(10)	7.66306(12)	7.68119(12)	7.69757(12)	7.71361(11)	7.72945(11)	7.74351(13)	7.75748(12)	7.77193(10)	7.78307(10)	7.79483(12)
V (Å^3)	223.843(5)	225.412(6)	226.797(6)	228.039(6)	229.289(6)	230.532(6)	231.750(8)	232.892(7)	234.013(6)	235.017(6)	235.987(7)
A											
x_A	0.9931(4)	0.9911(7)	0.9939(9)	0.9963(12)	0.9975(14)	0.9946(17)	0.9965(23)	0.9958(24)	0.9915(26)	0.9925(31)	0.9950(30)
y_A	0.0353(2)	0.0333(3)	0.0325(4)	0.0302(6)	0.0285(7)	0.0264(10)	0.0265(13)	0.0220(17)	0.0151(31)	0.0212(26)	0.0171(31)
z_A	1/4	1/4	1/4	1/4	1/4	1/4	1/4	1/4	1/4	1/4	1/4
d_A	0.519	0.531	0.540	0.558	0.571	0.584	0.583	0.615	0.655	0.615	0.635
x_A	0.0027	0.0013	0.0027	0.0050	0.0068	−0.0004	0.0015	0.0016	−0.0045	−0.0019	0.0006
y_A	−0.0953	−0.0974	−0.0989	−0.1018	−0.1040	−0.1065	−0.1062	−0.1117	−0.1188	−0.1115	−0.1150
B(Å^2)	0.52(2)	0.46(3)	0.85(3)	1.05(4)	1.17(4)	1.22(7)	1.25(7)	1.34(8)	1.64(10)	1.21(12)	1.02(12)
B											
x_B	0	0	0	0	0	0	0	0	0	0	0
y_B	1/2	1/2	1/2	1/2	1/2	1/2	1/2	1/2	1/2	1/2	1/2
z_B	0	0	0	0	0	0	0	0	0	0	0
B(Å^2)	0.21(2)	0.09(2)	0.34(2)	0.40(2)	0.40(1)	0.36(1)	0.44(2)	0.35(1)	0.32(1)	0.23(12)	0.12(1)
O1											
x	0.0701(8)	0.0715(12)	0.0649(14)	0.0702(16)	0.0682(16)	0.0643(17)	0.0595(21)	0.0616(21)	0.0576(21)	0.0596(23)	0.0645(62)
y	0.4839(6)	0.4818(11)	0.4846(14)	0.4863(17)	0.4868(21)	0.4880(27)	0.4899(34)	0.4909(41)	0.4926(62)	0.4883(55)	0.4939(24)
z	1/4	1/4	1/4	1/4	1/4	1/4	1/4	1/4	1/4	1/4	1/4
B(Å^2)	0.18(9)	0.30(7)	1.28(9)	0.68(8)	0.46(8)	0.68(10)	0.37(11)	0.24(11)	0.54(13)	0.41(13)	0.50(11)
O2											
x	0.7114(5)	0.7093(8)	0.7147(11)	0.7153(12)	0.7127(11)	0.7300(18)	0.7302(21)	0.7268(20)	0.7340(26)	0.7264(23)	0.7275(25)
y	0.2887(5)	0.2911(8)	0.2909(10)	0.2917(11)	0.2935(11)	0.2937(13)	0.2909(16)	0.2941(16)	0.2929(18)	0.2917(20)	0.2845(21)
z	0.0372(4)	0.0404(7)	0.0384(8)	0.0370(8)	0.0363(8)	0.0369(10)	0.0372(11)	0.0387(11)	0.0372(11)	0.0370(12)	0.0309(15)
B(Å^2)	0.39(6)	0.30(7)	1.28(9)	0.68(8)	0.46(8)	0.68(10)	0.37(11)	0.24(11)	0.54(13)	0.41(13)	0.50(13)
R_{wp}	12.84	9.60	7.70	7.08	6.61	6.79	7.19	6.95	7.18	7.43	6.52
R_{exp}	10.06	7.12	5.92	5.27	4.88	4.63	4.85	4.27	4.18	4.11	4.01
χ^2	1.28	1.35	1.30	1.34	1.35	1.47	1.48	1.63	1.72	1.80	1.62
R_{Bragg}	2.79	2.80	2.47	2.11	2.14	1.83	1.99	1.79	2.34	1.88	1.56
DW	1.39	1.24	1.28	1.23	1.19	1.08	1.04	0.86	0.79	0.74	0.86
GoF	1.28	1.35	1.30	1.34	1.36	1.47	1.48	1.63	1.72	1.81	1.62

Note: Standard deviations are given in parentheses. t—Goldschmidt tolerance factor; $^{viii}t_o$—observed tolerance factor in assumption of ^{viii}A coordination. x_A and y_A—parameters in fractions of the unit cell dimensions (a, b) describing displacement of A-site cation from the center of coordination polyhedron, d_A (Å).

the longest A–^{II}O(2) bond and the minimum A–B distance (Table 3, Fig. 4a). In addition, we have repeatedly synthesized compounds with $x = 0.3-0.5$, and found no statistically significant differences in their crystal structures that would negate our conclusions. Over the compositional range $x = 0.5-0.7$, the B cations remain in close proximity to the second coordination sphere as illustrated by insignificant changes in the A–^{II}O(2)$_{max}$ bond lengths for these compounds (Table 3; Fig. 4a). The actual coordination number of these compounds is ambiguous. However, with further increases in x, the B-cations move further from the A-site coordination sphere, as demonstrated by the increase in the separation between the longest A–^{II}O(2) bond and the A–B interatom distance. This trend culminates with the attainment of 9-fold coordination in pure $NaTaO_3$, although the coordination of the $0.7 \leqslant x \leqslant 0.9$ compounds remains ambiguous.

The volume of the first coordination sphere (AO_8) increases regularly throughout the series, with the exception of the $x = 0.4$ compound which has an anomalously small AO_8 volume (Table 2, Fig. 4b). The volume of the second coordination sphere ($[\Delta V = V(AO_{12}) - V(AO_8)]$; Table 2; Fig. 4b) increases throughout the whole series and has a local maximum for the $x = 0.4$ compound. The coincidence of these anomalies with exit of the B-cation from the second coordination sphere suggests interactions of the B-site

Table 2
Crystal chemistry of $Ca_{1-x}Na_xTi_{1-x}Ta_xO_3$

	AO_8	Δ_8	A–O(1)	A–O(2)	BO_6	Δ_6	B–O	f-8	ΔV	AO_{12}	f-12	[110]	[001]	[111]	a_x^-
$CaTiO_3$	25.273(6)	2.502	2.521(3)	3.136(6)	9.953(2)	0.007	1.954(2)	2.54	20.73	46.01	4.62	11.45	9.01	14.53	8.11
$x=0.1$	25.308(9)	3.227	2.522(6)	3.157(6)	10.096(4)	0.010	1.964(4)	2.51	20.95	46.26	4.58	11.75	9.96	15.36	8.32
$x=0.2$	25.600(12)	3.139	2.538(7)	3.133(8)	10.058(5)	0.108	1.962(4)	2.55	21.04	46.64	4.64	10.65	9.62	14.31	7.54
$x=0.3$	25.899(13)	2.899	2.544(8)	3.134(9)	10.128(6)	0.151	1.966(5)	2.54	21.20	46.88	4.63	11.40	8.91	14.43	8.07
$x=0.4$	25.387(13)	3.103	2.551(9)	3.135(10)	10.191(6)	0.124	1.970(5)	2.49	21.74	47.13	4.63	11.05	9.45	14.50	7.83
$x=0.5$	25.962(18)	2.706	2.569(12)	3.107(12)	10.110(8)	1.460	1.967(6)	2.57	21.56	47.52	4.70	10.45	8.23	13.27	7.40
$x=0.6$	26.246(22)	2.474	2.579(14)	3.098(15)	10.128(9)	1.159	1.968(7)	2.59	21.56	47.81	4.72	9.65	8.51	12.84	6.83
$x=0.7$	26.267(26)	3.247	2.583(15)	3.105(16)	10.238(9)	1.140	1.975(7)	2.57	21.72	47.98	4.69	9.95	9.30	13.59	7.04
$x=0.8$	26.492(32)	3.515	2.605(17)	3.066(19)	10.195(11)	1.854	1.973(9)	2.60	21.82	48.31	4.74	9.30	8.58	12.63	6.58
$x=0.9$	26.599(33)	3.045	2.593(17)	3.105(21)	10.298(11)	0.850	1.978(9)	2.58	21.86	48.46	4.71	9.60	8.93	13.08	6.79
$NaTaO_3$	26.972(38)	2.604	2.613(20)	3.068(24)	10.271(14)	0.390	1.975(10)	2.63	21.75	48.73	4.74	10.35	6.14	12.02	7.33

Note: AO_8 and AO_{12} volumes (Å^3) of polyhedra with A-site cation in 8 and 12-fold coordination, respectively. BO_6 is the volume (Å^3) of the BO_6 polyhedron. Δ_8 and Δ_6 are the distortion indices of the AO_8 and BO_6 polyhedra, respectively. AO_{12} the ideal volume of the A-site polyhedron which is calculated from V and BO_6. A–O^i and B–O are the mean bond lengths (Å) for the AO_8 and BO_6 polyhedra, respectively, A–O(1) first and A–O(2) second coordination spheres of A cation. The volume of the second coordination sphere, ΔV, is AO_{12}–AO_8. Polyhedron volume ratios (V_A/V_B), f-12 and f-8, are for 8 and 12-fold coordinated A-site cations, respectively. [110], [001] and [111] are octahedral tilts angles (deg) and a_x^- is the [100]=[010] tilt angle (deg); all tilt angles are determined from bond angles.

Table 3
Selected interatomic distances (Å) and angles (deg) in $Ca_{1-x}Na_xTi_{1-x}Ta_xO_3$

	$CaTiO_3$	$x=0.1$	$x=0.2$	$x=0.3$	$x=0.4$	$x=0.5$	$x=0.6$	$x=0.7$	$x=0.8$	$x=0.9$	$NaTaO_3$
A–O1	2.367(5)	2.376(7)	2.378(6)	2.360(11)	2.368(12)	2.408(13)	2.428(17)	2.422(17)	2.468(18)	2.458(21)	2.418(22)
A–O1	2.477(4)	2.484(6)	2.400(9)	2.527(10)	2.539(12)	2.560(16)	2.568(20)	2.604(19)	2.655(35)	2.603(34)	2.661(38)
2 x A–O2	2.379(3)	2.344(5)	2.378(6)	2.388(7)	2.382(8)	2.415(10)	2.432(12)	2.395(12)	2.398(14)	2.406(16)	2.461(17)
2 x A–O2	2.616(3)	2.621(5)	2.629(7)	2.655(8)	2.682(7)	2.633(10)	2.632(12)	2.661(13)	2.657(14)	2.664(16)	2.692(18)
2 x A–O2	2.668(3)	2.693(5)	2.695(6)	2.690(7)	2.686(8)	2.744(9)	2.752(11)	2.762(11)	2.803(13)	2.774(14)	2.760(15)
A–O1	3.030(4)	3.038(6)	3.017(8)	3.001(10)	2.992(12)	2.978(16)	2.967(20)	2.943(24)	2.901(35)	2.963(34)	2.915(38)
A–O1	3.044(5)	3.048(7)	3.032(9)	3.078(11)	3.079(12)	3.046(13)	3.036(17)	3.047(17)	3.004(17)	3.027(21)	3.069(22)
2 x A–$O2_{max}$	3.234(3)	3.270(5)	3.242(6)	3.228(7)	3.234(8)	3.201(9)	3.194(12)	3.214(12)	3.180(13)	3.215(15)	3.144(16)
2 x A–B_{min}	3.166(2)	3.186(1)	3.195(2)	3.210(2)	3.223(2)	3.238(4)	3.242(6)	3.267(8)	3.304(8)	3.292(13)	3.303(13)
2 x B–O1	1.949(1)	1.957(1)	1.942(6)	1.938(6)	1.946(6)	1.875(9)	1.888(10)	1.896(10)	1.871(13)	1.910(12)	1.925(15)
2 x B–O2	1.953(3)	1.963(4)	1.954(1)	1.963(2)	1.965(2)	1.965(2)	1.964(2)	1.969(2)	1.969(2)	1.973(2)	1.981(2)
2 x B–O2	1.961(3)	1.972(4)	1.990(6)	1.997(6)	1.999(6)	2.059(8)	2.052(10)	2.059(10)	2.079(12)	2.051(12)	2.020(14)
O1–B–O1	180	180	180	180	180	180	180	180	180	180	180
2 x O1–B–O2	89.1(1)	88.5(2)	88.2(3)	89.3(3)	89.3(3)	88.3(4)	87.8(5)	87.9(5)	87.6(7)	87.8(6)	90.7(7)
2 x O1–B–O2	89.7(1)	90.0(1)	90.4(2)	89.8(3)	90.0(3)	91.7(4)	92.2(5)	92.1(5)	92.3(7)	92.2(6)	89.7(7)
2 x O1–B–O2	90.9(1)	91.5(2)	91.8(3)	90.7(3)	90.7(3)	89.9(4)	91.4(5)	88.8(5)	91.5(6)	90.7(6)	90.3(7)
2 x O1–B–O2	90.3(1)	90.0(1)	89.6(2)	90.2(3)	90.1(3)	91.4(5)	89.1(5)	88.5(5)	88.7(7)	88.7(7)	89.7(7)
2 x O2–B–O2	90.6(2)	9.0.7(3)	90.9(3)	90.9(4)	90.9(4)	90.1(4)	87.7(5)	91.5(5)	91.3(7)	91.3(7)	90.3(7)
2 x O2–B–O2	89.4(2)	89.1(3)	89.1(3)	89.1(4)	89.1(4)	88.6(5)	90.9(5)	91.2(5)	88.5(6)	89.3(6)	89.3(7)
B–O1–B	157.1	156.5	158.7	157.2	157.9	159.1	160.7	160.1	161.4	160.6	159.5
B–O2–B	155.8	154.1	155.6	156.0	155.5	157.9	158.2	156.7	158.4	157.6	160.9
δ	0.36	0.83	1.20	0.38	0.37	1.44	2.65	2.31	2.70	2.01	0.19

Note: Δ bond angle variance (see text and [1] for explanation).

cations with the most distant O(2) anions of the second coordination sphere of the A-site cation, and an increase in coordination number. Similar trends are evident for coordination polyhedra in ternary orthorhombic lanthanide ferrites. For example, Marezio et al. [6], and Marezio and Dernier [25], have shown that with increasing ionic radius of the A-site cation in lanthanide orthoferrites that the coordination of this site is eight for compounds ranging from Lu to Sm, ambiguous for $PrFeO_3$ and $NdFeO_3$, and nine-fold for $LaFeO_3$. Similar trends are found for the lanthanide orthoscandates [18]. As far as we are aware, our present study is the first to report this phenomenon arising from coupled substitutions involving both the A- and B-site cations.

We employ the Δ_n distortion index introduced by Shannon [23] to illustrate polyhedron bond length

distortion, given as $\Delta n = \frac{1}{n} \cdot \sum\{(r_i - \bar{r})/\bar{r}\}^2 \times 10^3$, where r_i and $\bar{r}$ are individual and average bond lengths in the polyhedron, respectively. The distortion indices for the coordination polyhedra are summarized in Table 2. To characterize deviations from the ideal bond angles in regular octahedra, we calculate the bond angle variance index, δ_n, where $\delta_n = \sum[(\theta_I - 90)^2/(n-1)]$, and θ_i are the bond angles at the central atom. The bond angle variation indices are listed in Table 3.

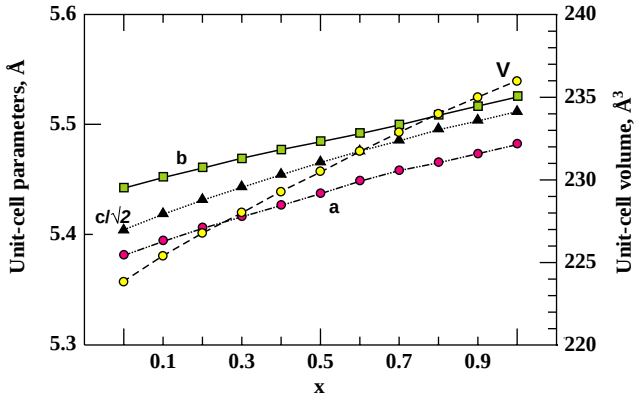

Fig. 3. Variation of unit-cell parameters and volumes in the $Ca_{1-x}Na_xTi_{1-x}Ta_xO_3$ solid solution series. Note: error bars are less than a dot size employed for plotting (Table 1).

Values of the distortion indices of the AO_8 coordination polyhedra (Δ_8) in most members of the $CaTiO_3$–$NaTaO_3$ solid solution series are close to those calculated for $CaTiO_3$, $GdFeO_3$ and other orthoferrites [18]. On the whole, the Δ_8 distortion index varies insignificantly, from 2.502 to 3.515, with local maxima at $x = 0.4$ and 0.8 (Fig. 4b). The [a, −b, 0]-displacement of the A cations from the center of AO_8 coordination polyhedron, d_A, increases with x (Fig. 4b) and shows minima for compounds with $x = 0.6$, 0.9 and 1.0.

The distortion of the BO_6 octahedron (Δ_6) is also controlled by interaction of the B cation with the second coordination sphere of the A cation. Evolution of this parameter with x (Fig. 5a) is non-linear. For compounds in which the B-site cations remains within the second coordination sphere of the A-site cations, this increases slightly and regularly from near zero, for the $CaTiO_3$ end member, to 0.124 for the $x = 0.4$ compound (Table 2; Fig. 5a). For compounds with $0.4 < x \leqslant 0.8$, the magnitude of the distortion increases by a factor of

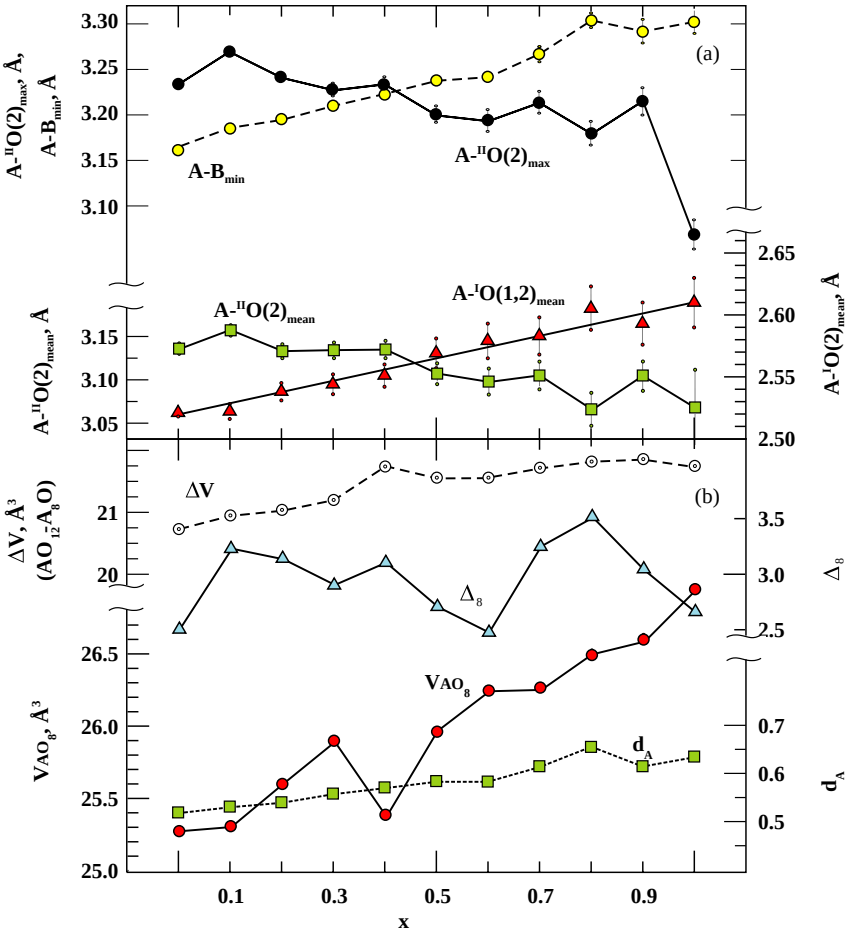

Fig. 4. Variation of bond lengths and polyhedral volumes in the $Ca_{1-x}Na_xTi_{1-x}Ta_xO_3$ solid solution series. Note: where not seen, the error bars are less than a dot size employed for plotting (Table 1).

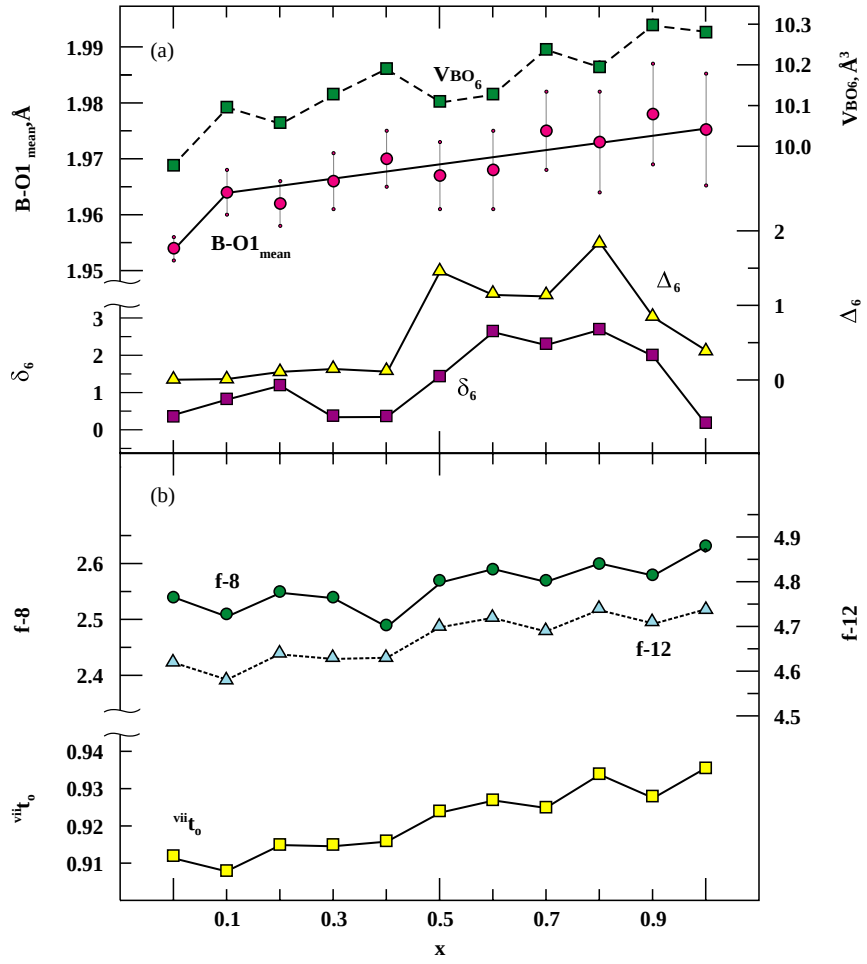

Fig. 5. Variation of bond lengths and polyhedral volume ratios in the $Ca_{1-x}Na_xTi_{1-x}Ta_xO_3$ solid solution series. *Note*: where not seen, the error bars are less than a dot size employed for plotting (Table 1).

10, followed by a decrease to 0.84 and 0.39 for the BO_6 octahedra in the $x = 0.9$ and $NaTaO_3$ compounds, respectively. The lesser distortion of these latter compounds can be attributed to the increasing distance between the *B*-site cation and the closest $^{II}O(2)$ anions. Octahedral bond angle distortion (δ_6) also shows similar complex evolution (Fig. 5a) and is minimal for the end member compositions.

Polyhedron volume ratios ($f = V_A/V_B$), increase irregularly throughout the series both for AO_8 and AO_{12} volumes (*f*-8 and *f*-12, respectively; Fig. 5b), with the clearly developed minima for both parameters at $x = 0.4$. Observed eight-fold tolerance factors ($^{viii}t_o$) increase with increasing values of x (Fig. 5b) but show no anomalies at x=0.4.

Octahedral tilt angles are less than described for lanthanide orthoferrites and orthoscandates [5,6,18], and decrease, in accord with decreasing *f*-parameters, with the replacement of $CaTiO_3$ by $NaTaO_3$ (Table 2). All of the octahedron tilts of the $Ca_{0.1}Na_{0.9}Ti_{0.1}Ta_{0.9}O_3$ and $NaTaO_3$ compounds are much closer to each other as compared to other members of the series. Unlike other crystallochemical parameters, the different modes of tilting do not exhibit any significant response to the interactions of the *B* cation with the second coordination sphere of the *A* cation.

Marezio et al. [6] have formulated empirical reasons for the anomalous crystallochemical characteristics observed in the lanthanide orthoferrite series of perovskites, although a quantitative model describing these anomalies has not yet been developed. It has been noted that among the 12 A–$^{I,II}O$ distances in the *Pbnm* orthoperovskites, the bond lengths in the first coordination sphere increase coincidently with the increase of $^{viii}R_A$ of the cations from heavy to light lanthanides, whereas A–$^{II}O(2)$ distances for the second coordination sphere decrease. As is evident from Fig. 4a, these trends are also observed for the $Ca_{1-x}Na_xTi_{1-x}Ta_xO_3$ series. The change of the second nearest neighborhood bond lengths in compounds with larger $^{viii}R_A$ is ascribed to "the screening effect of the first-nearest oxygen anions on the second-nearest oxygen anions" [6]. The atom in

the *B*-site, entering the second coordination sphere, also provides a screening effect. The latter becomes prominent when A–$^{II}O(2)$ bond lengths became considerably longer than that those of *A*–*B* distance, resulting in *B*-cations lying closer to the *A*-site atom than the most-distant couple of $^{II}O(2)$ anions. This steric effect occurs in the ternary $GdFeO_3$-type perovskites with the least-distorted BO_6 polyhedra due to the relatively small average radii of cations filling the *B* positions, which do not differ significantly from $^{vi}R^{4+}_{Ti}$ (Table 1).

4. Conclusion

The series of complex $Ca_{1-x}Na_xTi_{1-x}Ta_xO_3$ oxides have been synthesized at ambient pressure in air by ceramic techniques and their structures have been determined by Rietveld refinement of powder X-ray diffraction data at room temperature. These ternary stoichiometric perovskites, in common with $GdFeO_3$ and $CaTiO_3$, adopt space group *Pbnm*, and consist of distorted coordination polyhedra of both *A* and *B* cations. Deviation from cubic symmetry occurs in response to the tilting of the BO_6 polyhedra.

Because of the coincidence of the increase in the average ionic radii of both of the *A*- and *B*-site cations through the series, the Goldschmidt tolerance factor, *t*, does not change significantly (Table 1), and is close to 0.89, throughout the whole series. In terms of the observed tolerance factor, $^{viii}t_o$ [5], the distortion of the perovskite structure is less regular, but increases with *x* from 0.912 to 0.936 (Fig. 5b) assuming, for comparative purposes, eight fold coordination of the *A*-site cations.

Our data confirm the existence of a complete isostructural (*Pbnm*) solid solution between $CaTiO_3$ and $NaTaO_3$ at ambient temperature. The evolution of the crystallochemical characteristics throughout the series is complex as demonstrated by

(i) The interplay between the contemporaneous distortions of the *A*- and *B*-site coordination polyhedra;
(ii) Interactions of the *B*-site cation with the second coordination sphere of the *A* cation. *B*-site cations are inside the A–$^{II}O(2)$ coordination sphere for $x = 0$–0.4 but lie outside of this sphere for $x \geqslant 0.5$. *B*-site cations remain in the vicinity of the $^{II}O(2)$ anions in the compositional range of $x = 0.5$–1.0 although the interatom distances increase with *x*, and are greatest for $NaTaO_3$;
(iii) The coordination of the *A*-site cations changes throughout the series from eight for $CaTiO_3$ to nine-fold for $NaTaO_3$. Compounds with $0 \leqslant x \leqslant 0.4$ have *A*-site cations in eight fold coordination, whereas the coordination of those with $0.4 < x < 0.9$ is ambiguous.

Acknowledgments

This work is supported by the Natural Sciences and Engineering Research Council of Canada and Lakehead University. Mr. Alan MacKenzie is acknowledged for assistance with the X-ray diffraction and SEM EDS microprobe work, Mrs. Anne Hammond is warmly thanked for help with preparation of samples. Three reviewers for the *Journal of Solid State Chemistry* are thanked for their constructive comments.

References

[1] R.H. Buttner, E.N. Maslen, Acta Crystallogr. B 48 (1992) 644.
[2] S.A.T. Redfern, J. Phys.: Condens. Matter 8 (1996) 8267.
[3] B.J. Kennedy, C.H. Howard, B.C. Chakoumakos, J. Phys.: Condens. Matter 11 (1999) 1479.
[4] K. Leinenweber, J. Parise, Amer. Mineral. 82 (1997) 475.
[5] R.H. Mitchell, Perovskites: Modern and Ancient. Almaz Press, Thunder Bay, Ontario, Canada, 2002, 322pp. (http://www.almazpress.com).
[6] M. Marezio, J.P. Remeika, P.D. Dernier, Acta Crystallogr. B 26 (1970) 2008.
[7] J. Hutton, R.J. Nelmes, Acta Crystallogr. A 37 (1981) 916.
[8] A.M. Glazer, Acta Crystallogr. Sect. B 28 (1972) 3384.
[9] T.H. Yamanaka, N. Hirai, Y. Komatsu, Amer. Mineral. 87 (2002) 1183.
[10] C.J. Howard, R.L. Winters, B.J. Kennedy, J. Solid State Chem. 160 (2001) 8.
[11] R. Ranjan, D. Padney, V. Siruguri, P.R.S. Krishna, S.K. Paranjpe, J. Phys.: Condens. Matter 11 (1999) 2233.
[12] S. Quin, A.I. Becerro, F. Seifert, J. Gottsman, J. Jiang, J. Mater. Chem. 10 (2000) 1609.
[13] C.J. Ball, B.D. Begg, D.J. Cookson, G.J. Thorogood, E.R. Vance, J. Solid State Chem. 139 (1998) 238.
[14] B.J. Kennedy, A.K. Prodjosantoso, C.H. Howard, J. Phys.: Condens. Matter 11 (1999) 6319.
[15] C.N.W. Darlington, K.S. Knight, Acta Crystallogr. B 55 (1999) 24.
[16] N.E. Breese, M. O'Keefe, Acta Crystallogr. B 47 (1991) 192.
[17] I.D. Brown, D. Altermatt, Acta Crystallogr. B 41 (1985) 244.
[18] R.P. Liferovich, R.H. Mitchell, J. Solid State Chem. 177 (2004) 2188.
[19] A.A. Kern, A.A. Coelho, Allied Publishers Ltd., 1998, p. 144. http://www.bruker-axs.com.
[20] E. Dowty, Atoms 5.0, By Shape Software, Kingsport, TN 37663, USA, 1999.
[21] T. Balić-Žunić, I. Viković, J. Appl. Crystallogr. 29 (1996) 305.
[22] Y. Zhao, D.J. Weidner, J.B. Parise, D.E. Cox, Phys. Earth Planet. Interiors 76 (1993) 1.
[23] R.D. Shannon, Acta Crystallogr. Sect. A 32 (1976) 751.
[24] V.M. Goldschmidt, Skrifter Norsk. Vidensk. Akad. Klass. 1, 8 (1926) 2.
[25] M. Marezio, P.D. Dernier, Mater. Res. Bull. 6 (1971) 23.